

Excitation of high- n toroidicity-induced shear Alfvén eigenmodes by energetic particles and fusion alpha particles in tokamaks

G. Y. Fu and C. Z. Cheng

Princeton Plasma Physics Laboratory, Princeton University, Princeton, New Jersey 08543

(Received 3 June 1992; accepted 20 July 1992)

The stability of high- n toroidicity-induced shear Alfvén eigenmodes (TAE) in the presence of fusion alpha particles or energetic ions in tokamaks is investigated. The TAE modes are discrete in nature, and thus can easily tap the free energy associated with energetic particle pressure gradient through wave particle resonant interaction. A quadratic form is derived for the high- n TAE modes using gyrokinetic equation. The kinetic effects of energetic particles are calculated perturbatively using the ideal magnetohydrodynamic (MHD) solution as the lowest-order eigenfunction. The finite Larmor radius (FLR) effects and the finite drift orbit width (FDW) effects are included for both circulating and trapped energetic particles. It is shown that, for circulating particles, FLR and FDW effects have two opposite influences on the stability of the high- n TAE modes. First, they have the usual stabilizing effects by reducing the wave particle interaction strength. Second, they also have destabilizing effects by allowing more particles to resonate with the TAE modes. It is found that the growth rate induced by the circulating alpha particles increases linearly with the toroidal mode number n for small $k_{\theta}\rho_{\alpha}$, and decreases as $1/n$ for $k_{\theta}\rho_{\alpha} \gg 1$. The maximum growth rate is obtained at $k_{\theta}\rho_{\alpha}$ on the order of unity, and is nearly constant for the range of $0.7 < v_{\alpha}/v_A < 2.5$. On the other hand, the trapped particle response is dominated by the precessional drift resonance. The bounce resonant contribution is negligible. The growth rate peaks sharply at the value of $k_{\theta}\rho_{\alpha}$, such that the precessional drift resonance occurs for the most energetic trapped particles. The maximum growth rate due to the energetic trapped particles is comparable to that of circulating particles. Finally, the effect of the two-dimensional wave structure of TAE modes is considered by using the Wentzel-Kramers-Brillouin (WKB) method.

I. INTRODUCTION

As we are closer to the realization of tokamak plasma fusion ignition, it is extremely important to understand the novel behaviors of burning plasma associated with fusion product alpha particles. One subject, which has received increasing attention recently, is the alpha particle destabilization of shear Alfvén waves. It has been long recognized^{1,2} that shear Alfvén waves can be excited by tapping the free energy source associated with the energetic particle pressure gradient through parallel wave particle interaction. One particular class of shear Alfvén waves considered in this paper is the toroidicity-induced Alfvén eigenmode^{3,4} (TAE). Recently, interest in TAE modes has surged following theoretical predictions,⁵⁻¹⁰ and subsequent experimental evidences^{11,12} of their excitation by super-Alfvénic energetic particles. The growth rate γ of the TAE mode induced by energetic particles may be expressed in a generic local formula,

$$\frac{\gamma}{\omega_{\text{TAE}}} = q^2 \beta_h \left(\frac{\omega_{*}}{\omega_{\text{TAE}}} - 1 \right) f_r - \frac{\gamma_d}{\omega_{\text{TAE}}}, \quad (1)$$

where ω_{TAE} is the real part of the TAE eigenfrequency, β_h is the energetic particle (alpha particle) beta value, q is the tokamak safety factor, ω_{*} is the diamagnetic drift frequency of energetic particle, f_r is related to the fraction of the number of resonant particles, and finally, γ_d is the damping rate of the TAE mode due to core plasma kinetic

effects and Alfvén continuum damping.¹³⁻¹⁷ From this equation, it is clear that three conditions must be satisfied in order to destabilize the TAE mode. They are (1) the energetic particle speed must be comparable to the Alfvén phase speed v_A in order to allow the parallel wave-particle resonance to occur; (2) the energetic particle pressure gradient must be steep enough so that inverse Landau damping occurs, i.e., $\omega_{*}/\omega_{\text{TAE}} > 1$; and (3) the net energetic particle destabilizing contribution must overcome the background damping of the TAE mode. Recent theory^{5-10,13} and experimental evidences^{11,12} have shown that low- n TAE modes can be excited by neutral beam injected hot ions with a large β_h of the energetic particles. In an ignited tokamak plasma, the fusion product alpha particles have a birth velocity comparable or larger than the Alfvén phase velocity, and have a pressure profile sharply peaked at the center of the plasma. Therefore, the first and the second condition for destabilization of the TAE mode can be easily met. However, the third condition is not as easily satisfied for low- n TAE modes, since the alpha particle beta value β_{α} is relatively low, on an order of 1%.

In this work, we consider the excitation of high- n TAE modes by energetic ions or alpha particles. High- n TAE modes are expected to be more susceptible to the destabilization than the low- n modes. Note that, in Eq. (1), the energetic particle destabilizing term is proportional to ω_{*} , which is, in turn, proportional to the toroidal mode num-

ber n . Furthermore, recent work^{14,15} suggests that the Alfvén continuum damping of the TAE modes tends to decrease with increasing mode number n . On the other hand, the finite Larmor radius effects (FLR) and the finite drift orbit effects (FDW) are stabilizing, and are expected to increase with the mode number. Balance of these competing effects yields an intermediate mode number n for which the TAE mode is most susceptible to the energetic particle destabilization (or the smallest critical beta).

The energetic/alpha particle effects on high- n TAE modes have been studied previously.^{8,18–21} Chen⁸ considered alpha particle destabilization analytically for large aspect ratio low-beta model tokamak equilibria, in the limit of zero orbit width. Spong *et al.*¹⁸ studied the same problem for general numerical equilibria, but for trapped particles only. The finite orbit width was also neglected. Guo, Van Dam, and Wakatani¹⁹ also studied the trapped energetic particle effects on the TAE mode, but for a model equilibrium of divertor tokamaks. Recently, Rewoldt²⁰ studied the alpha particle effect on high- n Alfvén modes by using a more comprehensive approach, and found that an Alfvén branch can be destabilized by fusion alpha particles. The Alfvén mode had a real frequency $\omega_r \approx v_A/qR$, and may be related to the ellipticity-induced Alfvén eigenmodes.²² More recently, Berk, Breizman, and Ye²¹ were first to study analytically the effects of finite orbit excursion on the linear response of energetic particles to the TAE modes. It was found²¹ that the banana orbit effect reduces the power transfer by a factor of Δ_m/Δ_b when the banana width Δ_b is much larger than the mode thickness Δ_m . This result implies that the growth rate of the TAE mode induced by the energetic particles is *independent* of the mode number. However, our results indicate that the dependence of the mode number is still significant, even for large banana width. We find that the growth rate increases *continuously* as the mode number increases until it reaches its maximum and begins to decrease at $k_\perp \rho_a$ on the order of unity. The discrepancy comes from the oversimplification made in Ref. 21 by neglecting the radial dependence of the wave-particle resonance condition.

Our formulation retains full FLR effects and the main FDW effects by employing the gyrokinetic equation.^{23,24} We derive a quadratic form for the high- n TAE modes from the parallel and perpendicular components of Ampère's law and from the quasineutrality condition. We assume that the TAE modes can be described by the ideal magnetohydrodynamic (MHD) equation. Thus, we treat energetic particle effects perturbatively. We note that similar perturbative methods have been used previously^{6,10} in calculating the energetic particle effects on low- n TAE modes. The TAE eigenmode structure is obtained via the Wentzel-Kramers-Brillouin (WKB) method.^{14,16} The lowest-order WKB solution represents the fast radial variation for each poloidal mode, whereas the higher-order solution describes the slow radial variation of the amplitude, which naturally includes the physics of Alfvén continuum damping.^{14,15} We will first present the results in the local limit using the lowest-order WKB solution. The non-

local effects on the energetic particle destabilization will also be studied.

In Sec. II of the present paper, a perturbative formula for the growth rate induced by energetic particles is derived. In Sec. III we present numerical and analytical results for the destabilizing effects in the radially local limit due to fusion alpha particles, as well as the background damping effects due to thermal species. The effects of the nonlocal radial structures of the high- n TAE mode are considered in Sec. IV. Finally in Sec. V, discussions and conclusions are given.

II. FORMULATION

Here we derive a quadratic form for the high- n TAE modes with kinetic effects of the energetic particle, including fusion alpha particles, as well as background plasma species. We start with the standard gyrokinetic equation^{23,24} in terms of the WKB-ballooning formalism:

$$(\omega - \omega_d + i\sigma v_\parallel \mathbf{b} \cdot \nabla) g_j^\sigma = -q_j \frac{\partial F_j}{\partial E} (\omega - \omega_*) \left[J_0 \left(\phi - \sigma \frac{v_\parallel}{c} A_\parallel \right) + \frac{v_\perp}{c} A_\perp J_1 \right] + iC(g_j), \quad (2)$$

where g_j^σ is the nonadiabatic portion of the perturbed distribution function,

$$f_j = f_j \exp(iS - i\omega t), \quad (3)$$

and is given by

$$f_j = q_j \phi \left(\frac{\partial F_j}{\partial E} + \frac{1}{B} \frac{\partial F_j}{\partial \mu} \right) - q_j A_\parallel \frac{v_\parallel}{c} \frac{\partial F_j}{\partial \mu} + g_j \exp(iL). \quad (4)$$

In Eqs. (2)–(4), $J_l = J_l(|\nabla S| v_\perp / \Omega)$ is the l th-order Bessel function, S is the usual eikonal that describes the fast variation of the perturbed quantities perpendicular to the magnetic field line, and C is the gyroaveraged pitch angle scattering collision operator,²⁵ which is given in the zero Larmor radius limit by

$$C(g_j) = \nu \frac{m_j v_\parallel}{B} \frac{\partial}{\partial \mu} \left(v_\parallel \mu \frac{\partial g_j}{\partial \mu} \right). \quad (5)$$

This collision operator will only be used for electrons. Thus, it may be justified to adopt this form in the zero FLR limit. More definitions in Eqs. (2)–(4) are as follows. Here A_\parallel and A_\perp is the parallel and perpendicular component of the perturbed magnetic vector potential, respectively, ϕ is the perturbed electrostatic potential, ω is the wave frequency, \mathbf{b} is the unit vector of the equilibrium magnetic field, the subscript j denotes the particle species, F_j is the equilibrium particle distribution function, σ is the sign of the parallel velocity v_\parallel , E is the particle energy, $\mu = mv_\perp^2 / 2B$ is the magnetic moment, Ω is the cyclotron frequency, c is the speed of light, $L = \mathbf{b} \times \nabla S \cdot \mathbf{v} / \Omega$, and ν is the particle collision frequency. Finally, we list the definitions for the vector field \mathbf{A} , the magnetic drift frequency ω_d , and the diamagnetic drift frequency ω_* :

$$\mathbf{A} = A_\parallel \mathbf{b} - i \frac{\mathbf{b} \times \nabla S}{|\nabla S|} A_\perp, \quad (6)$$

$$\omega_d = -\mathbf{b} \times \nabla S \frac{mv_{\parallel}^2 \kappa + \mu \nabla B}{m\Omega}, \quad (7)$$

$$\omega_* = \frac{\mathbf{b} \times \nabla S \cdot \nabla F}{m\Omega \partial F / \partial E}, \quad (8)$$

where $\kappa = \mathbf{b} \cdot \nabla \mathbf{b}$ is the magnetic curvature. After substituting $A_{\parallel} \equiv (c/i\omega) \mathbf{b} \cdot \nabla \Phi$,

$$g_j \equiv -q_j \frac{\partial F_j}{\partial E} \left(1 - \frac{\omega_*}{\omega}\right) J_0 \Phi + h_j, \quad (9)$$

and the $\mathbf{b} \times \nabla S$ component of Ampère's law,

$$B_{\parallel} = \frac{4\pi}{\omega B^2} \mathbf{b} \times \nabla S \cdot \nabla P \Phi - B_1, \quad (10)$$

into Eq. (2), we obtain a convenient form of the gyrokinetic equation as follows:

$$(\omega - \omega_d + i\sigma v_{\parallel} \mathbf{b} \cdot \nabla) h_j^{\sigma} = -q_j \frac{\partial F_j}{\partial E} \left(1 - \frac{\omega_*}{\omega}\right) H^{\sigma}, \quad (11)$$

with H_j^{σ} being defined as

$$H^{\sigma} \equiv J_0(\omega \Psi + \omega_k \Phi) - J_2 \omega_p \Phi + i\sigma v_{\parallel} \mathbf{b} \cdot \nabla J_0 \\ - \frac{\omega v_1^2}{2\Omega c} (J_0 + J_2) B_1, \quad (12)$$

where we have made the following definitions:

$$\Psi = \phi - \Phi, \quad (13)$$

$$\omega_p = \frac{4\pi\mu}{qB} \mathbf{b} \times \nabla S \cdot \nabla P, \quad (14)$$

$$\omega_k = \omega_d - \omega_p, \quad (15)$$

$$B_1 = \frac{4\pi}{c} \sum_j q_j \int d^3v \frac{v_1^2}{2\Omega} (J_0 + J_2) h_j. \quad (16)$$

We can now proceed to derive the system of eigenmode equations from Eq. (11), the Ampère's law, and the quasineutrality condition. After multiplying Eq. (11) with $J_0 q_j$ on both sides, integrating over velocity space and summing over all species, we obtain

$$\frac{c^2}{4\pi\omega} \mathbf{b} \cdot \nabla \frac{|\nabla S|^2}{B^2} \mathbf{b} \cdot \nabla \Phi + \sum_j \int d^3v \omega (1 - J_0^2) \frac{q_j^2}{T_j} F_j \Phi \\ + \sum_j \omega \frac{n_j q_j^2}{T_j} \Psi \\ = - \sum_j \int d^3v q_j^2 \frac{\partial F_j}{\partial E} \left(1 - \frac{\omega_*}{\omega}\right) J_0 H^{\sigma} \\ + \sum_j \int d^3v q_j (J_0 \omega_d + i\sigma v_{\parallel} \mathbf{b} \cdot \nabla J_0) h_j^{\sigma}, \quad (17)$$

where we have used the parallel component of Ampère's law,

$$\sum_j \int d^3v q_j \sigma v_{\parallel} h_j^{\sigma} = -\frac{ic^2}{4\pi\omega} |\nabla S|^2 \mathbf{b} \cdot \nabla \Phi, \quad (18)$$

and the quasineutrality condition,

$$\sum_j \int d^3v q_j J_0 h_j = \sum_j \frac{n_j q_j^2}{T_j} \Psi + \sum_j \int d^3v (1 - J_0^2) \frac{q_j^2}{T_j} F_j \Phi. \quad (19)$$

We then expand the Bessel function J_0 in the second term of Eq. (17), by assuming small gyroradius ordering for thermal ions. Equation (17) becomes

$$\mathbf{b} \cdot \nabla \frac{|\nabla S|^2}{B^2} \mathbf{b} \cdot \nabla \Phi + \frac{\omega^2}{v_A^2} |\nabla S|^2 (\Phi + \Psi) - \frac{8\pi}{B^2} (\mathbf{b} \times \nabla S \cdot \nabla P) \\ \times (\mathbf{b} \times \nabla S \cdot \kappa) \Phi \\ = \sum_j \frac{4\pi\omega}{c^2} \int d^3v q_j (J_0 \omega_k - J_2 \omega_p + i\sigma v_{\parallel} \mathbf{b} \cdot \nabla J_0) h_j^{\sigma}. \quad (20)$$

Equations (11), (16), (19), and (20) constitute our system of eigenmode equations for four unknown fields: h_j^{σ} , Φ , Ψ , and B_1 .

We now derive a quadratic form from this set of eigenmode equations in order to facilitate our perturbative calculation of the TAE growth rate induced by energetic particles. To do this, we multiply Eq. (16) with $\omega^2 B_1^*/c^2$, Eq. (19) with $4\pi\omega^2 \Psi^*/c^2$ and Eq. (20) with Φ^* , add them together, and integrate along the field line. After integration by parts, we obtain

$$\int \frac{dl}{B} Q(\Phi, \Psi, B_1) = 0, \quad (21)$$

where

$$Q(\Phi, \Psi, B_1) \\ = |\nabla S|^2 |\mathbf{b} \cdot \nabla \Phi|^2 + \frac{8\pi}{B^2} (\mathbf{b} \times \nabla S \cdot \nabla P) (\mathbf{b} \times \nabla S \cdot \kappa) |\Phi|^2 \\ - \omega^2 \frac{|\nabla S|^2}{v_A^2} |\Phi|^2 - \omega^2 \frac{|\nabla S|^2}{v_A^2} (\Phi^* \Psi + \Phi \Psi^*) \\ + \frac{\omega^2}{c^2} |B_1|^2 - \sum_j 4\pi \frac{\omega^2 n_j q_j^2}{c^2 T_j} |\Psi|^2 \\ + \sum_j 4\pi \frac{\omega}{c^2} \int d^3v q_j (H^{\sigma})^* h_j^{\sigma}. \quad (22)$$

Our derivation of Eq. (22) is similar to that of Xu and Rosenbluth,²⁶ but with one important difference: that we retain full FLR effects. Note the first three terms in Eq. (22) constitute the ideal MHD equation without compression effects (i.e., the B_1 term) and kinetic effects (i.e., the parallel electric field term Ψ and the nonadiabatic h_j).

The kinetic terms in Eq. (22) can be shown to be small compared to ideal MHD terms as follows. First, we need to solve for h_j in Eq. (11), and then to solve for Ψ in Eq. (19). For thermal ions, the lowest-order solution to Eq. (11) is $h_i \approx q_i F_i / T_i (\Psi + \omega_k / \omega \Phi)$ for $\omega \gg \omega_{c,i}$ where $\omega_{c,i}$ is the ion transit frequency. For thermal electrons, the main contribution to h_e comes from the trapped particles, since $\omega \ll \omega_{c,e}$ and the lowest-order solution is $h_e = \langle h_e \rangle \approx (qF_e / T_e) \omega_k / \omega \langle \Phi \rangle$, where $\langle \rangle$ denotes the bounce average. We can now solve Eq. (19) to obtain Ψ . We first note that the electron contribution to the left-hand

side can be neglected because the trapped particle population is small. Second, the alpha particle terms in Eq. (19) can also be dropped, since its density is assumed to be small. Plugging h_i into the equation and expanding the Bessel function for ion species, we obtain $\Psi = (T_e/T_i)[-1/2(k_1 \rho_i)^2 + \hat{\omega}_k/\omega]\Phi$, where the overbar denotes the average over the equilibrium particle distribution function. This expression for Ψ will be used in the calculation of the electron collisional damping. We can now proceed to compare the kinetic terms with the MHD inertial term in Eq. (22). The fourth term of the Eq. (22) is small, as compared to the MHD inertial term, since $k_1 \rho_i \ll 1$ and $\omega_k/\omega \ll 1$. The sixth term is also small due to the ordering $k_1 \rho_i \ll 1$ and $\omega_{c,i} \ll \omega$. Finally, the last term in Eq. (22) is small since the beta value for each species is assumed to be small.

The growth rate due to kinetic effects can now be calculated perturbatively. Let $\omega = \omega_0 + \delta\omega$ and $\Phi = \Phi_0 + \delta\Phi$, where ω_0 and Φ_0 denotes the ideal eigenfrequency and eigenfunction, respectively; the δ terms are the corresponding small kinetic corrections. Using this ordering, the quadratic form can be expanded and the lowest-order terms [the first three terms in Eq. (22)] yield the following ideal MHD equation for Φ_0 :

$$\mathbf{B} \cdot \nabla \frac{|\nabla S|^2}{B^2} \mathbf{B} \cdot \nabla \Phi_0 + \frac{\omega^2}{v_A^2} |\nabla S|^2 \Phi_0 - \frac{8\pi}{B^2} (\mathbf{b} \times \nabla S \cdot \nabla P) \times (\mathbf{b} \times \nabla S \cdot \kappa) \Phi_0 = 0. \quad (23)$$

The next-order equation determines $\delta\omega$, which is given by

$$\frac{\delta\omega}{\omega} = \frac{\sum_j N_j}{W}, \quad (24)$$

where

$$N_j = \frac{2\pi}{\omega_0 c^2} \int \frac{dl}{B} \int d^3v q_j(H^\sigma) * h_j, \quad (25)$$

$$W = \int \frac{dl}{B} \frac{|\nabla S|^2}{v_A^2} \Phi_0^2. \quad (26)$$

Here N_j represents the kinetic contribution due to particle species j , which includes the energetic particle, as well as thermal electrons and ions. Note that we have only included the contribution of the last term in Eq. (22) to $\delta\omega$ since we are only interested in the growth rate.

We now solve Eq. (11) for h_j^σ . The solution for the circulating particles is

$$h_j^\sigma = q_j \frac{\partial F_j}{\partial E} \left(1 - \frac{\omega_*}{\omega}\right) \times \int_{-\infty}^{+\infty} dk \frac{H^\sigma(k) \exp[ik\theta_c - i\sigma I_c(\theta)]}{\sigma k \omega_c - \omega}, \quad (27)$$

where

$$H^\sigma(k) = \int_{-\infty}^{+\infty} d\theta_c \exp[-ik\theta_c + i\sigma I_c(\theta)] H^\sigma(\theta), \quad (28)$$

$$\theta_c = \omega_c \int_0^\theta \frac{JB}{v_\parallel} d\theta, \quad (29)$$

$$I_c(\theta) = \int_0^\theta \omega_d \frac{JB}{v_\parallel} d\theta, \quad (30)$$

and ω_c is the transit frequency of the circulating particles. The solution for trapped particles is

$$h_j^\sigma = \frac{V_j^+(\theta_m) + V_j^-(\theta_m)}{2 \sin[\bar{I}_b(\theta_m)]} \exp[i\sigma \bar{I}_b(\theta)] - i\sigma V_j^\sigma(\theta), \quad (31)$$

where

$$V_j^\sigma(\theta) = \int_{-\pi/2}^{\theta_b} d\theta'_b H^\sigma \exp\{-i\sigma[\bar{I}_b(\theta') - \bar{I}_b(\theta)]\}, \quad (32)$$

$$\bar{I}_b(\theta) = \int_{-\theta_m}^\theta \frac{JB}{v_\parallel} d\theta(\omega - \omega_d), \quad (33)$$

$$\theta_b = \omega_b \int_{-\theta_m}^\theta \frac{JB}{v_\parallel} d\theta' - \frac{\pi}{2}. \quad (34)$$

Here, ω_b is the bounce frequency of the trapped particles, θ_m is the poloidal angle corresponding to the turning point of the banana orbit, θ_b is the bounce angle, and J is the coordinate transform Jacobian. Finally, we list a useful formula to be used in calculating the resonant contribution of the trapped particles:

$$\begin{aligned} \text{Res} \left[\oint d\theta_b (H^\sigma) * h_j^\sigma \right] &= \frac{2}{\omega_b} \cot[\bar{I}_b(\theta_m)] \left| \oint d\theta_b H_1 \cos[\bar{I}_b(\theta)] \right. \\ &\quad \left. + H_2 \sin[\bar{I}_b(\theta)] \right|^2 \\ &= -2i \sum_p |H_p^l|^2 \delta(\omega - p\omega_b - \bar{\omega}_d), \end{aligned} \quad (35)$$

where $H^\sigma \equiv H_1 + i\sigma H_2$, Res denotes the resonant part of the contribution and

$$H_p^l = \oint d\theta_b \{H_1(\theta) \cos[p(\theta_b + \pi/2) - I_b(\theta)] + H_2(\theta) \sin[p(\theta_b + \pi/2) - I_b(\theta)]\}, \quad (36)$$

$$I_b(\theta) = \int_{-\theta_m}^\theta (\omega_d - \bar{\omega}_d) \frac{JB}{v_\parallel} d\theta. \quad (37)$$

Here the bounce integration for H_p^l is done at the l th trapped particle region, namely $2\pi l - \theta_m < \theta < 2\pi l + \theta_m$.

After plugging h_j^σ into Eq. (24) for both circulating particles and trapped particles, the growth rate $\gamma = -i \delta\omega$ can be determined straightforwardly, and is given by

$$\frac{\gamma}{\omega_0} = \sum_j \frac{2\pi^2 \int E dE (-q_j^2 \partial F_j / \partial E) (\omega_* / \omega_0 - 1) (N_j^h + N_j^t)}{m_j^2 c^2 B^2 \omega_0 \int_{-\infty}^{+\infty} (|\nabla S|^2 \Phi_0^2 J / v_A^2) d\theta}, \quad (38)$$

where J is the coordinate transform Jacobian, N_j^u and N_j^t represents the contribution due to circulating particles and trapped particles, respectively, and

$$N_j^u = \int_0^{\Lambda_1} d\Lambda \int_{-\infty}^{+\infty} dk \frac{1}{\omega_c} [|H^+(k)|^2 + |H^-(k)|^2] \times \delta(k\omega_c - \omega), \quad (39)$$

$$N_j^t = \int_{\Lambda_1}^{\Lambda_2} d\Lambda \sum_{l,p=-\infty}^{+\infty} \frac{1}{\omega_b} |H_p^l|^2 \delta(p\omega_b + \bar{\omega}_d - \omega). \quad (40)$$

In Eqs. (39) and (40), $H^\pm(\mp k)$ is the Fourier transformation of $H^\sigma(\theta)$ for circulating particles, $\bar{\omega}_d$ is the bounce-averaged magnetic drift frequency, and $\Lambda = \mu B_0 / E$ is the particle velocity pitch angle variable, with Λ_1 corresponding to the trapped and circulating boundary and Λ_2 corresponding to the deeply trapped particles.

III. NUMERICAL AND ANALYTICAL RESULTS: LOCAL THEORY

In this section, we evaluate the growth rate of the high- n TAE mode due to energetic particles and the damping due to thermal electrons and ions in the local limit. By the local limit, we mean that the eigenfunction Φ is approximated by the lowest-order WKB solution. In general, the WKB solution can be written as

$$\Phi = A(r)\Phi(r,\theta)\exp(inS), \quad (41)$$

where $S = \zeta - q(r)\theta$ is the WKB eikonal, θ and ζ are the poloidal and toroidal angle, respectively, and r is the magnetic flux variable and is a measure of the mean radius. In Eq. (41), $\exp(inS)$ describes the fast variation of the TAE mode across the field line, and $\Phi(r,\theta)$ describes the slow variation along the field line and is determined by the lowest-order WKB equation; whereas $A(r)$ describes the slow variation of the radial envelope for these poloidal modes, and is determined by the higher-order WKB equation.¹⁶ In the lowest order, $A(r)$ is constant. In this section, we calculate the growth rate according to Eq. (38) in this local limit. The results with correction due to the nonlocal higher-order terms will be presented in the next section.

Although our formulation is valid for general noncircular tokamak equilibria, We consider large aspect ratio, low-beta model equilibria²⁷ with shifted circular magnetic surfaces, in order to simplify our problem. For this model equilibrium, the ideal MHD equation [Eq. (23)] becomes the well-known high- n ballooning mode equation:²⁷

$$\frac{\partial}{\partial \theta} G(\theta) [1 + h^2(\theta)] \frac{\partial}{\partial \theta} \Phi + \bar{\omega}^2 G(\theta) (1 + 4\epsilon \cos \theta) \times [1 + h^2(\theta)] \Phi + \Delta_p [\cos \theta + h(\theta) \sin \theta] \Phi = 0, \quad (42)$$

where $h(\theta) = s(\theta - \theta_k) - \Delta_p \sin \theta$, $G(\theta) = 1 + 2\Delta' \cos \theta$, $s = q dq/q dr$, $\Delta_p = -2q^2 R (dP/dr) / B^2$, Δ' is the radial derivative of the Shafranov shift, $\epsilon = r/R$, and $\bar{\omega} = \omega/\omega_A$, with $\omega_A = v_A/qR$ being the Alfvén frequency. Finally, θ_k is the

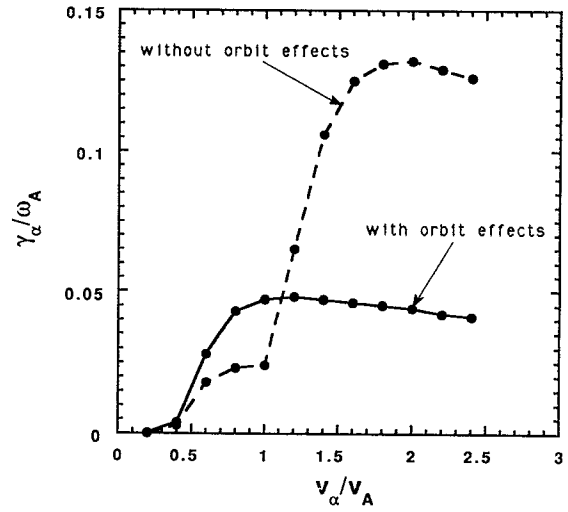


FIG. 1. Growth rates induced by circulating alpha particles as a function of v_α/v_A for $s=0.6$, $\Delta_p=0$, and $k_{\theta\alpha}=1.0$.

radial wave number that describes the slow radial variation. For our local limit assumed here, θ_k is chosen to be zero.

In this work, we mainly consider fusion alpha particles. The particle distribution function is described by a slowing-down energy distribution with uniform pitch angle. We will consider the contributions from circulating particles and trapped particles separately. The key parameters are v_α/v_A (the ratio of alpha birth speed to Alfvén phase velocity) and $k_{\theta\alpha}$ (the finite orbit width parameter), where the Larmor radius is defined with the birth alpha velocity. Finally, we model the alpha particle density profile as $n_\alpha(r) = n_\alpha(0) \exp[-(r/L_\alpha)^2]$, where L_α is the density scale length. To obtain the alpha particle induced growth rate, we first obtain the numerical solutions of Eq. (42) for Φ by shooting method. The boundary conditions are $\Phi(\pm\infty) = 0$. After we obtain Φ , we plug it into Eq. (38) to calculate the growth rate perturbatively. For circulating particle contribution, we perform numerical integration in θ , k , and Λ ; the energy integration can be done analytically due to the resonant δ function. For the trapped particle contribution, we first carry out integration in θ_b for the l th trapped region, then sum up l and the bounce harmonic p , and finally carry out the pitch angle integration.

In Sec. III A, we will calculate the destabilizing contribution of the circulating alpha particles, while in Sec. III B, we will consider the destabilizing contribution of the trapped alpha particles. Section III C is devoted to the damping rates of the TAE mode due to thermal particle species. Finally, in Sec. III D, we evaluate the critical beam beta value for the excitation of the TAE mode in the Tokamak Fusion Test Reactor (TFTR) neutral beam injection (NBI) experiment.¹¹

A. Circulating particle contribution

We first consider the destabilizing contribution of circulating alpha particles. The parameters of $\epsilon=0.1$, $q=1.0$, $L_p/R=0.1$, and $\beta_\alpha(0)=2\%$ are chosen. Figure 1 shows

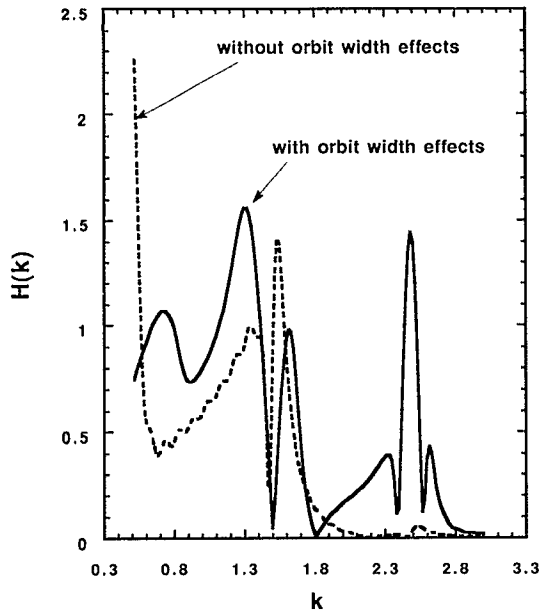


FIG. 2. Function $H(k)$ for $s=0.6$, $\Delta_p=0$, $v_\alpha/v_A=1.0$, and $k_{\theta\rho_\alpha}=1.0$.

the growth rates induced by circulating alpha particles as a function of v_α/v_A for parameters of $s=0.6$ and $\Delta_p=0.0$ and $k_{\theta\rho_\alpha}=1.0$. The dashed curve is obtained in the limit of zero orbit width [i.e., the FLR and the FDW effects are turned off in Eq. (39), but $\omega_* \propto k_{\theta\rho_\alpha}$ is kept finite]. The solid curve corresponds to the results with finite orbit width effects. We see that the finite orbit effects are stabilizing for $v_\alpha/v_A > 1.1$ and destabilizing for $v_\alpha/v_A < 1.1$. This exhibits two opposite influences of finite orbit size. On one hand, finite orbit width has a stabilizing effect by reducing the wave-particle interaction strength; on the other hand, this orbit width effect has a destabilizing effect by bringing more particles into resonance with the waves. Figure 2 shows function $H^+(k)$ with and without orbit width effects at the resonant energy. Physically, $H(k)$ is related to the work done on the resonant particles by the perturbed electrical field, and k is related to the radial variable $nq - m$ for the poloidal mode number m . Thus, $H(k)$ is a measure of the strength of the wave-particle interaction as a function of the radius. Figure 2 shows that, in the limit of zero orbit width, $H(k)$ peaks sharply at $k=\frac{1}{2}$ and $k=\frac{3}{2}$, reflecting the fact that the TAE mode peaks at $nq - m = \pm 1/2$ magnetic surfaces with a radial localization width on the order of $\epsilon r/n$. However, with finite orbit width effects, $H(k)$ is shown to have a much broader peak, with a smaller amplitude near $k=\frac{1}{2}$ (Note that an additional peak appears at $k=\frac{3}{2}$ due to the poloidal mode coupling induced by the magnetic drift orbit.) Physically, these broader peaks mean that particles away from where mode localizes can still interact effectively with the mode due to the finite orbit width effects. It is clear that the destabilizing effect of the finite orbit width is a direct consequence of the radially localized structure of the TAE mode.

We now study the variation of the growth rate as a function of $k_{\theta\rho_\alpha}$. It is known that without orbit width effects, the growth rate is a linear function of $k_{\theta\rho_\alpha}$. However,

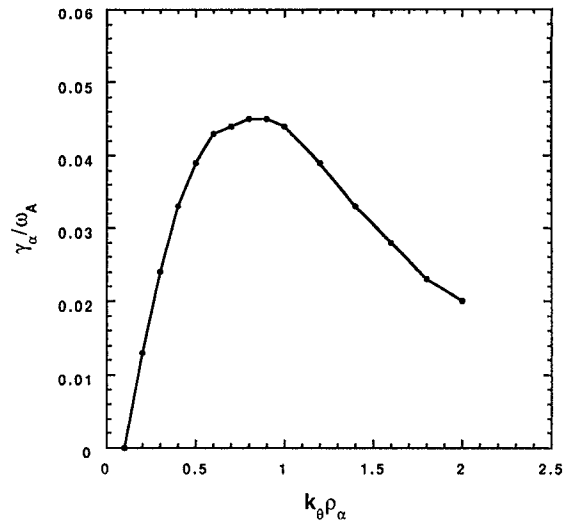


FIG. 3. Growth rate induced by circulating alpha particles as a function of $k_{\theta\rho_\alpha}$ for $s=0.6$, $\Delta_p=0$, and $v_\alpha/v_A=2.0$.

this linear dependence is expected to be modified by the finite orbit width. Figure 3 shows the growth rate as a function of $k_{\theta\rho_\alpha}$ with orbit width effects for parameters of $s=0.6$, $\Delta_p=0$, and $v_\alpha/v_A=2.0$. We observe that as $k_{\theta\rho_\alpha}$ increases, the growth rate first increases linearly, then saturates at $k_{\theta\rho_\alpha}=0.8$, and finally decreases for $k_{\theta\rho_\alpha} > 1.0$. Note that the value of $k_{\theta\rho_\alpha}$ that maximizes the growth rate is on an order of unity. Naively, one would expect that $(k_{\theta\rho_\alpha})_{\max}$ is on the order of unity and $(k_{\theta\rho_\alpha})_{\max}$ is on the order of $\epsilon = r/R$. We note that our numerical results differs significantly from that of Ref. 21. First, our results show that the growth rate is maximized at $k_{\theta\rho_\alpha}$ on an order of unity instead of $k_{\theta\rho_\alpha} \ll 1$, as implied in Ref. 21. Second, we have shown that the growth rate eventually decreases as a function of $k_{\theta\rho_\alpha}$ for $k_{\theta\rho_\alpha} \gg 1$, whereas the results of Ref. 21 imply a constant growth rate for $k_{\theta\rho_\alpha} \gg \Gamma$. Next, we consider the variation of $(k_{\theta\rho_\alpha})_{\max}$ and the corresponding $(\gamma_\alpha/\omega_A)_{\max}$ with v_α/v_A , as shown in Fig. 4, for parameters of $s=0.6$ and $\Delta_p=0$. We see that $(k_{\theta\rho_\alpha})_{\max}$ decrease as v_α/v_A increases, and $(\gamma_\alpha/\omega_A)_{\max}$ is nearly constant in the range of $0.7 < v_\alpha/v_A < 2.0$.

Next, we study the effects of the magnetic shear s and the curvature-pressure-gradient parameter Δ_p on TAE stability. For $s=0.6$ and $\Delta_p=0$, the high- n TAE mode frequency is about at the center of the Alfvén continuum gap,³ which corresponds to the most global radial wave structure. As s and Δ_p varies, the eigenfrequency shifts toward either the bottom or the upper edge of the continuum gap, and its eigenfunction becomes more localized in the radial space²⁸ (or more extended in the Fourier θ space). Figure 5 shows $(k_{\theta\rho_\alpha})_{\max}$ and $(\gamma_\alpha/\omega_A)_{\max}$ as a function of s for $\Delta_p=0$. First, it is evident that $(k_{\theta\rho_\alpha})_{\max}$ is not sensitive to the magnetic shear. Second, the maximum growth rate peaks at $s=0.6$. It has been shown³ for the $\Delta_p=0$ case that as the magnetic shear decreases (increases) from $s=0.6$, the mode frequency decreases (increases) toward the bottom (top) edge of the continuum gap and the eigenfunction becomes increasingly localized

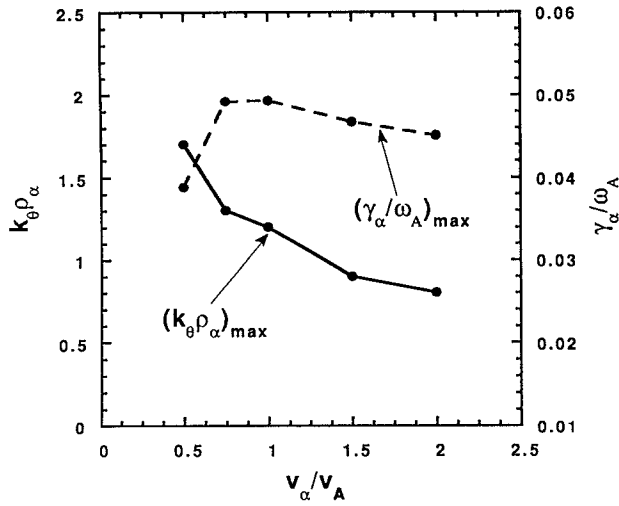


FIG. 4. The maximized growth rate induced by circulating alpha particles and the corresponding $k_{\theta\rho_{\alpha}}$ as a function of v_{α}/v_A for $s=0.6$ and $\Delta_p=0$.

in the real space. Physically, Fig. 5 indicates that the growth rate becomes smaller as the mode becomes more localized. This tendency is confirmed by the result of Fig. 6, which plots $(\gamma_{\alpha}/\omega_A)_{\alpha}$ and $(k_{\theta\rho_{\alpha}})_{\max}$ as a function of Δ_p at $s=0.6$. We see that the growth rate decreases as Δ_p increases, whereas $(k_{\theta\rho_{\alpha}})_{\max}$ is nearly constant. This is related to the fact²⁸ that the TAE eigenfrequency shifts downward to the bottom edge of the continuum gap as Δ_p increases. In particular, the TAE mode merges into the continuum and becomes singular when $\Delta_p > (\Delta_p)_{\text{crit}} = 0.225$, where $(\Delta_p)_{\text{crit}}$ is the critical value for the existence of the discrete TAE mode. It can be analytically shown that the growth rate tends to zero as Δ_p approaches $(\Delta_p)_{\text{crit}}$.

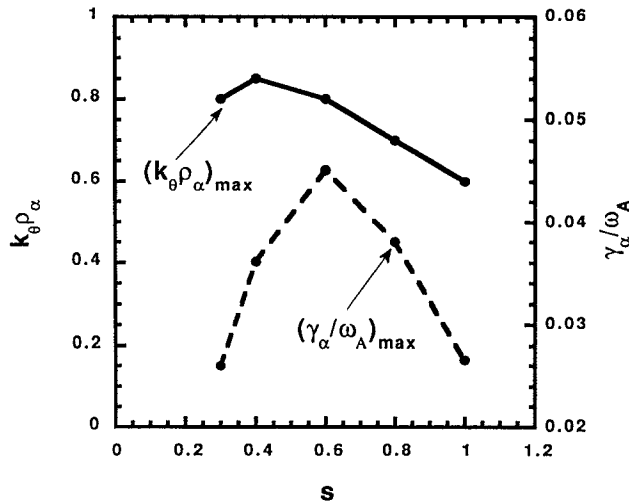


FIG. 5. The maximized growth rate induced by circulating alpha particles and the corresponding $k_{\theta\rho_{\alpha}}$ as a function of magnetic shear s for $\Delta_p=0.0$ and $v_{\alpha}/v_A=2$.

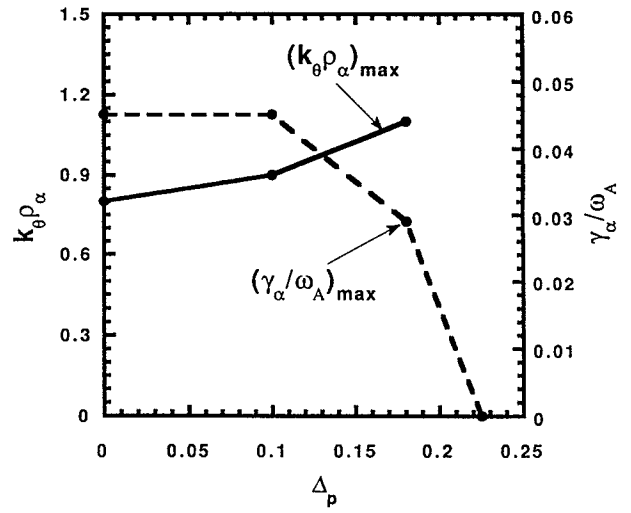


FIG. 6. The maximized growth rate induced by circulating alpha particles and the corresponding $k_{\theta\rho_{\alpha}}$ as a function of the pressure gradient parameter Δ_p for $s=0.6$ and $v_{\alpha}/v_A=2$.

The numerical results shown above for the circulating particles can be understood analytically in certain asymptotic limits. To simplify our analytic derivation, we normalize function $H(\theta)$ into a dimensionless form, such that

$$\bar{H}(\theta) = \frac{qBR}{cEk_{\theta}} H(\theta). \quad (43)$$

The function $H(k)$ and H_p^l is normalized in the same way as $\bar{H}(k)$ and \bar{H}_p^l , respectively. To make analytic progress, we consider the case of zero pitch angle. Also, we use an asymptotic form^{3,28} to approximate the high- n TAE solution:

$$\Phi_0(\theta) = \frac{\cos(\theta/2) + \lambda \sin(\theta/2)}{\sqrt{1 + (s\theta - \alpha \sin \theta)^2}} \exp(-\Gamma\theta), \quad (44)$$

where $\lambda = \Omega_+/\Omega_- \sim O(1)$, $\Gamma = \Omega_+ \Omega_- \sim O(\epsilon)$, and $\Omega_{\pm} = \pm [\bar{\omega}^2(1 + \bar{\epsilon}) - \frac{1}{4}]$, with $\bar{\epsilon} = 2.5\epsilon$ in the low beta limit. We can then compute $H(k)$ in the limit of zero orbit size, and obtain

$$\bar{H}(k) \approx \frac{\lambda\Gamma + \frac{1}{2} - k}{(\frac{1}{2} - k)^2 + \Gamma^2} + \frac{-\lambda\Gamma + \frac{3}{2} - k}{(\frac{3}{2} - k)^2 + \Gamma^2}, \quad (45)$$

where we have made use of the fact that the secular term $s\theta$ makes a dominating contribution in the limit of $\Gamma \ll 1$. Note that $\bar{H}(k)$ peaks at $k = \frac{1}{2}$ and $k = \frac{3}{2}$ with a narrow width of $\Gamma \sim O(\epsilon)$. This analytic result agrees with the numerical result shown in Fig. 2 (dashed curve). Using Eq. (45), the growth rate can be written into a simple form as

$$\frac{\gamma}{\omega_0} = \frac{3\pi}{8} q^2 \beta_h \frac{\omega_*}{\omega_0} \left[\left(\frac{v_A}{v_{\parallel}} \right)^4 \Theta \left(1 - \frac{v_A}{v_{\parallel}} \right) + \left(\frac{v_A}{3v_{\parallel}} \right)^4 \Theta \left(1 - \frac{v_A}{3v_{\parallel}} \right) \right], \quad (46)$$

where Θ is the Heaviside step function. This result is similar to the results obtained by Chen.⁸

We now consider the case with finite orbit width effects. We note that the gyroradius is zero for the zero pitch angle assumed here, but the particles can deviate from magnetic field lines due to the finite radial magnetic drift. This drift effect is contained in the secular term of the drift phase $I_c(\theta)$ in Eq. (30). To make analytic progress, we take the asymptotic limit $1 > k_{\theta} \rho_{\alpha} \gg \Gamma$ and $\Lambda \ll 1$. In this limit, the secular term in $\bar{H}(\theta)$ dominates the contribution to the integral $\bar{H}(k)$. We may then take the asymptotic form of $I_c(\theta)$ for large θ and expand in Bessel functions:

$$\exp[iI_c(\theta)] \approx J_0(z\theta) + 2 \sum_l (-i)^l J_l(z\theta) \cos(l\theta), \quad (47)$$

where $z = \bar{v}_{\parallel} k_{\theta} \rho_{\alpha}$ with $\bar{v}_{\parallel} = v_{\parallel} / v_{\alpha} \leq 1$. By keeping only the principle resonance term (i.e., for k near $\frac{1}{2}$), the integral $\bar{H}(k)$ then reduces to

$$\bar{H}(k) = \frac{2}{z} \left[\frac{\bar{k}}{z} + \lambda \sqrt{1 - \left(\frac{\bar{k}}{z}\right)^2} \right], \quad (48)$$

for $|\bar{k}| < z$, where $\bar{k} = \frac{1}{2} - k$ and

$$\bar{H}(k) = \frac{2}{z} \operatorname{sgn}(\bar{k}) \left[\frac{|\bar{k}|}{z} - \sqrt{\left(\frac{\bar{k}}{z}\right)^2 - 1} \right], \quad (49)$$

for $|\bar{k}| > z$. Equations (48) and (49) show that the peak of $\bar{H}(k)$ at $k = \frac{1}{2}$ now has a width on an order of $k_{\theta} \rho_{\alpha} \gg \Gamma$. Thus the width of the peak is broadened by the finite orbit width effects. This result agrees with the numerical result shown in Fig. 2. In the limit case of $1 \gg k_{\theta} \rho_{\alpha} \gg \Gamma$, the k integration in Eq. (38) can be carried out analytically, and the resulting growth rate is independent of $k_{\theta} \rho_{\alpha}$ or the mode number.²¹ However, for finite $k_{\theta} \rho_{\alpha}$ on an order of unity, the k integration has to be done numerically due to the energy dependence in z and $H(k)$. Our numerical result in Fig. 3 indicates that, as $k_{\theta} \rho_{\alpha}$ increases from zero, the growth rate first increases linearly as a function of $k_{\theta} \rho_{\alpha}$ for small $k_{\theta} \rho_{\alpha}$, then it reaches its maximum at $k_{\theta} \rho_{\alpha}$ on the order of unity, and finally decreases for $k_{\theta} \rho_{\alpha} > 1$. The decrease in the growth rate for $k_{\theta} \rho_{\alpha} \gg 1$ can be understood analytically in the following way. After integrating in energy, the growth rate given by Eq. (38) is proportional to the following k integral: $k_{\theta} \rho_{\alpha} \int_{k_m}^{\infty} (k_m/k)^4 [H(k)]^2 dk$. Since $H(k)$ scales as $1/k_{\theta} \rho_{\alpha}$ in the limit of $k_{\theta} \rho_{\alpha} \gg 1$ due to the fast drift phase $I_c(\theta)$, the growth rate scales as $1/k_{\theta} \rho_{\alpha}$ asymptotically for $k_{\theta} \rho_{\alpha} \gg 1$.

B. Trapped particle contribution

Here we consider the trapped energetic particle contribution to the growth rate of the TAE mode. As in the last section, we study the finite orbit width effects and the dependence of the growth rate on v_{α}/v_A , $k_{\theta} \rho_{\alpha}$, s , and Δ_p . The same fixed parameters of ϵ , q , L_p/R , and $\beta_{\alpha}(0)$ are used. First, we demonstrate the finite orbit width effects. Figure 7 shows the growth rates as a function of v_{α}/v_A with or without orbit width effects, for $s=0.6$, $\Delta_p=0$, and $k_{\theta} \rho_{\alpha}=1.0$. In the limit of zero orbit width, we turn off the FLR term contained in the Bessel functions and the finite banana width term contained in the drift phase term $I_d(\theta)$

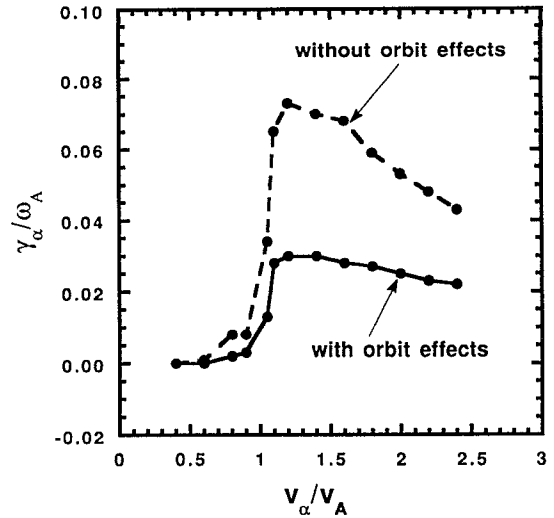


FIG. 7. Growth rates induced by trapped alpha particles as a function of v_{α}/v_A for $s=0.6$, $\Delta_p=0$, and $k_{\theta} \rho_{\alpha}=1.0$.

in Eq. (40), but we still keep the ω_{*} and $\bar{\omega}_d$ terms. We see that the growth rate is always reduced by the finite orbit width effect, in contrast with that of circulating particles. Furthermore, there is a sharp transition in the growth rate at $v_{\alpha}/v_A = 1.0$. Physically, the transition occurs at the precessional drift resonance $\bar{\omega}_d \approx \omega$. Note that the precessional drift resonance condition for deeply trapped particles is given by $k_{\theta} \rho_{\alpha} E \approx v_A/v_{\alpha}$, where $E \leq 1$ is the particle energy normalized to the birth energy of the alpha particle. Thus, for the parameters of Fig. 7, the precessional resonance can be satisfied for $v_{\alpha}/v_A \geq 1.0$. We also find that the bounce resonance contribution is much smaller than the precessional resonance contribution. This result has been confirmed in Ref. 29. It is also borne out by the result of Fig. 8, which shows the normalized growth rate as a function of $k_{\theta} \rho_{\alpha}$ for parameters of $s=0.6$, $\Delta_p=0$, and $v_{\alpha}/v_A=2.0$. We

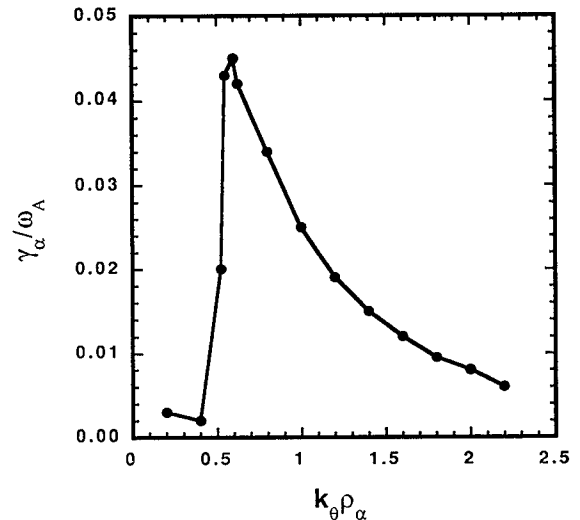


FIG. 8. Growth rate induced by trapped alpha particles as a function of $k_{\theta} \rho_{\alpha}$ for $s=0.6$, $\Delta_p=0$, and $v_{\alpha}/v_A=2.0$.

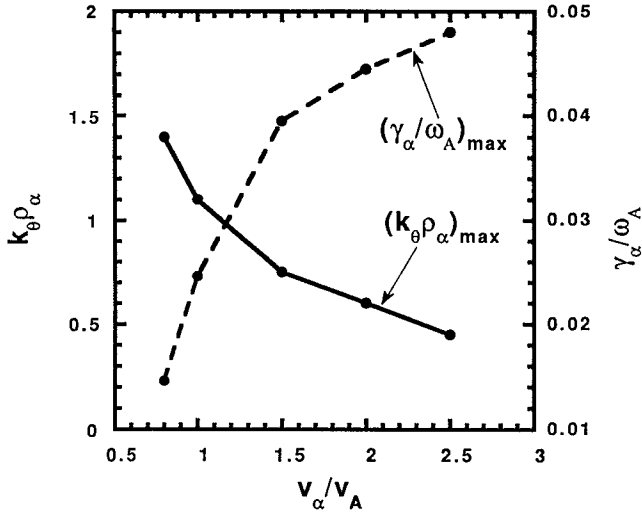


FIG. 9. The maximized growth rate induced by trapped alpha particles and the corresponding $k_{\theta\rho\alpha}$ as a function of v_{α}/v_A for $s=0.6$ and $\Delta_p=0$.

notice from Fig. 8 that the sharp transition occurs at $k_{\theta\rho\alpha} \approx 0.5$, precisely when the precessional drift resonance begins to occur. We also see that the growth rate then decreases rapidly due to the finite orbit width effect. The maximum growth rate is comparable to that of circulating particles, as shown in Fig. 3, but the growth rate is much more narrowly peaked at $k_{\theta\rho\alpha} \approx 0.6$.

We now study the dependence of $(k_{\theta\rho\alpha})_{\max}$ and $(\gamma_{\alpha}/\omega_A)_{\max}$ on v_{α}/v_A , as shown in Fig. 9, obtained for parameters of $s=0.6$ and $\Delta_p=0$. We observe that the maximum growth rate increases with v_{α}/v_A , and the increase is more gradual for larger values of v_{α}/v_A . On the other hand, $(k_{\theta\rho\alpha})_{\max}$ decreases with v_{α}/v_A , which agrees with our analytic result of $(k_{\theta\rho\alpha})_{\max} = v_A/v_{\alpha}$. Finally, their dependence on the magnetic shear s and the curvature-pressure-

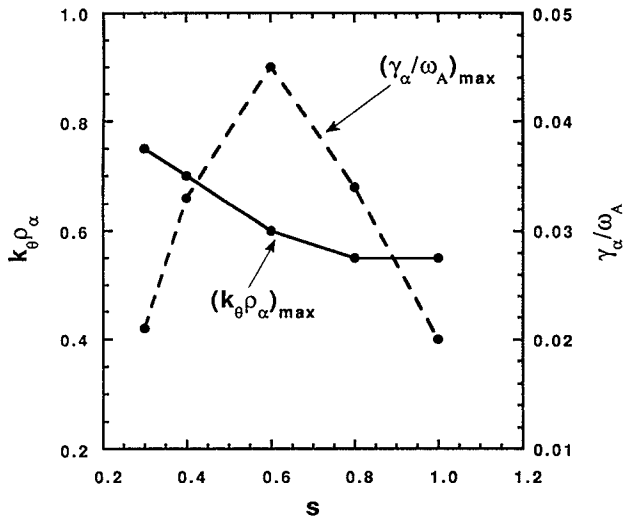


FIG. 10. The maximized growth rate induced by trapped alpha particles and the corresponding $k_{\theta\rho\alpha}$ as a function of magnetic shear s for $\Delta_p=0.0$ and $v_{\alpha}/v_A=2$.

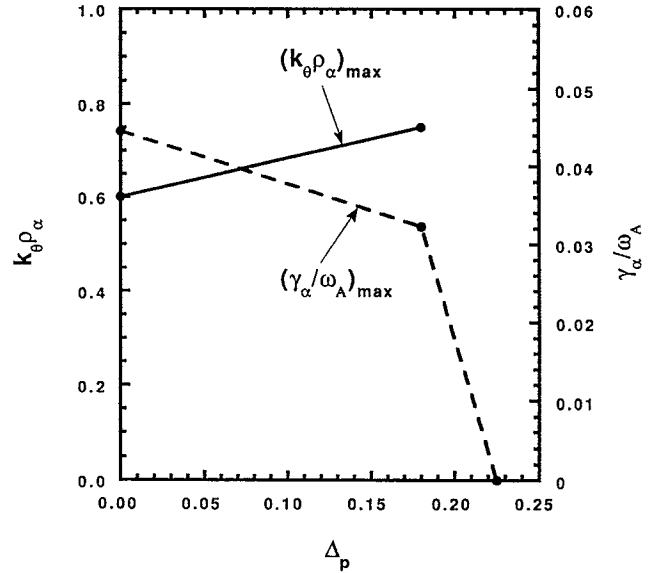


FIG. 11. The maximized growth rate induced by trapped alpha particles and the corresponding $k_{\theta\rho\alpha}$ as a function of the pressure gradient parameter Δ_p for $s=0.6$ and $v_{\alpha}/v_A=2$.

gradient parameter Δ_p are shown in Figs. 10 and 11. Overall results are similar to those for circulating particles.

Next, we derive analytic results for trapped particle contribution. We will demonstrate that the bounce resonance contribution of the trapped alpha particles is much smaller than the precession resonance contribution. We first consider the limit of zero orbit width. For even bounce harmonic p (including $p=0$), we obtain

$$\bar{H}_p^0 \approx \cos\left(\frac{\pi}{2}p\right) \oint d\theta_b \cos\frac{\theta}{2} [\cos\theta + (s\theta - \alpha \sin\theta)\sin\theta] \cos(p\theta_b), \quad (50)$$

$$\bar{H}_p^{l \neq 0} \approx \lambda \exp(-2\pi\Gamma l) \cos\left(\frac{\pi}{2}p\right) \times \oint d\theta_b \sin\theta \sin\frac{\theta}{2} \cos(p\theta_b); \quad (51)$$

while for odd p , we obtain $\bar{H}_p^0=0$ and

$$\bar{H}_p^{l \neq 0} \approx \exp(-2\pi\Gamma l) \sin\left(\frac{\pi}{2}p\right) \times \oint d\theta_b \sin\theta \cos\frac{\theta}{2} \sin(p\theta_b). \quad (52)$$

It is then straightforward to demonstrate that $(\bar{H}_0^0)^2 \gg 2\Sigma_l (\bar{H}_{p \neq 0}^l)^2$ (i.e., the precessional drift resonance contribution is much greater than the bounce contribution) for the deeply trapped particles. For finite pitch angle and very small Γ , the bounce contribution may be comparable to that of precessional drift resonance. However, the bounce contribution can be dramatically reduced by the effect of finite banana width. Therefore, the precession resonance dominates for *all* pitch angles.

We now consider the case with a finite orbit width effect. To make analytic progress, we examine the limit of deeply trapped particles. In this limit, we have shown that $\bar{H}_0^0 \gg \bar{H}_0^{l \neq 0}$, thus we may keep only the contribution from the $l=0$ trapped particle region. After some algebra, we obtain

$$\frac{\gamma_\alpha}{\omega_0} \approx \frac{3}{2} \sqrt{\frac{\epsilon}{2}} q^2 \beta_\alpha \frac{[(\omega_0/\bar{\omega}_{dm})^2 (\omega_*/\omega_0)] - \frac{3}{2} (\omega_0/\bar{\omega}_{dm})}{\int_0^\infty d\theta [1+h^2(\theta)] \Phi_0^2} (\bar{H}_0^0)^2, \quad (53)$$

for $\bar{\omega}_{dm} \gg \omega_0$, where $\bar{\omega}_{dm}$ is the maximum precessional drift frequency. Here \bar{H}_0^0 can be straightforwardly calculated to obtain

$$\bar{H}_0^0 \approx \pi J_0 \left(\sqrt{k_\theta \rho_\alpha \frac{\omega_0}{\bar{\omega}_{dm}}} \right). \quad (54)$$

After calculating the θ integration in the denominator by using the asymptotic form for the eigenfunction Φ_0 , Eq. (53) becomes

$$\frac{\gamma_\alpha}{\omega_0} \approx \frac{3\sqrt{2\epsilon}}{2G(\bar{\omega})} \pi^2 q^2 \beta_\alpha \left(\frac{r}{L_p} \right)^2 \{J_0[\sqrt{(k_\theta \rho_\alpha)_{\max} k_\theta \rho_\alpha}]\}^2 \times \frac{(k_\theta \rho_\alpha)_{\max}}{k_\theta \rho_\alpha}, \quad (55)$$

where $(k_\theta \rho_\alpha)_{\max} \approx v_A/qv_\alpha$ and $G(\bar{\omega}) = (1+\lambda^2)/(4\epsilon\Gamma) \sim O(1)$. This analytic result for the trapped particle contribution agrees very well with our numerical results [e.g., Fig. (8)].

C. Damping due to thermal particle species

Here we consider the stabilizing effects due to thermal particle species. We first consider the damping rate due to thermal ions. We note that the thermal speed v_i is, in general, much smaller than v_A , thus the $v_{\parallel} = v_A/3$ sideband resonance is dominating over the principle resonance. Also, the finite orbit effects may be neglected since $k_\theta \rho_i \ll 1$. Using the results of Eq. (45), the damping rate can then be straightforwardly derived to obtain

$$\frac{\gamma_i}{\omega_0} \approx \sqrt{\pi} q^2 \beta_i (1+x^2) x^3 \exp(-x^2), \quad (56)$$

where $x = v_A/3v_i$. Note that we have used the Maxwellian distribution for ions. This analytical expression agrees very well with our numerical results. We observe that the damping rate increases rapidly with ion beta due to the exponential dependence. For $q=1$, we find $\gamma_i/\omega_0 \geq 1\%$ for $\beta_i \geq 2\%$. Therefore, the ion damping could be substantial for moderately high ion beta value.

Next, we consider the damping rate of high- n TAE mode due to thermal electrons. It has been shown that the usual electron Landau damping is very small, since thermal electron velocity is much larger than the Alfvén velocity for typical tokamak parameters. Mikhailovskii and Shuchman,³⁰ and also Gorelenkov and Sharapov,³¹ showed that the dominating damping mechanism due to thermal electrons is the collisionality of trapped particles. Here, we

derive the damping rate of the high- n TAE mode induced by the collisionality of trapped electrons. We start from Eq. (11) for electrons. After neglecting small electron gyroradius and substituting Ψ in terms of Φ using the quasineutrality condition, Eq. (11) becomes

$$(\omega - i\nu_{\parallel} \mathbf{b} \cdot \nabla - iC) h_e^\sigma = q_e \frac{F_e}{T_e} H_e, \quad (57)$$

with

$$H_e = \left(-\frac{\omega |\nabla S|^2 \bar{m}_i}{2\Omega_e^2 m_e^2} T_e + \omega_k - \hat{\omega}_k \right) \Phi, \quad (58)$$

where $\hat{\omega}_k$ is the electron curvature drift frequency averaged over the Maxwellian distribution function. Note that in Eq. (58), the thermal ion FLR effect is kept to include the finite parallel electric field. To solve Eq. (57), we expand h_e in terms of the small parameter $\omega/\omega_b \ll 1$. The zeroth-order equation reads as $\mathbf{b} \cdot \nabla h_{e0} = 0$, which implies that h_{e0} is constant along the field lines, whereas the next-order terms yield

$$(\omega - i\langle C \rangle) h_{e0} = q_e \frac{F_e}{T_e} \langle H_e \rangle, \quad (59)$$

where $\langle \rangle$ denotes the average over the banana orbit and $\langle C \rangle$ is the bounce-averaged collisional operator, given by²⁵

$$\langle C \rangle = 2\bar{\nu} \left(\frac{E}{T_e} \right)^{-3/2} \frac{Z_{\text{eff}} + \Pi(E/T_e)}{\oint d\theta / \sqrt{1-\Lambda B}} \frac{\partial}{\partial \Lambda} \Lambda \oint d\theta \sqrt{1-\Lambda B} \frac{\partial}{\partial \Lambda}, \quad (60)$$

with the function $\Pi(z)$ being defined as

$$\Pi(z) = \frac{1}{\sqrt{\pi z}} e^{-z^2} + \left(1 - \frac{1}{2z^2} \right) \frac{z}{\sqrt{\pi}} \int_0^z e^{-t^2} dt, \quad (61)$$

where $\bar{\nu}$ is a normalized electron collision frequency, and is given by $\bar{\nu} = 4\pi n_e e^4 \ln \Lambda / (m_e^2 v_e^3)$. Following Rosenbluth *et al.*,²⁵ we solve Eq. (59) in the limit of $\bar{\nu}/\omega \ll 1$ and obtain an approximate solution, given by

$$h_{e0} \approx q_e \frac{F_e}{\omega T_e} (1 - e^{i\sqrt{D}\xi}) \langle H_e \rangle, \quad (62)$$

with

$$D = i \frac{\omega \epsilon \pi}{2\bar{\nu} \omega_b} \left(\frac{E}{T_e} \right)^{3/2} \frac{1}{Z_{\text{eff}} + \Pi(E/T_e)}, \quad (63)$$

where $\xi = (\Lambda - 1 + \epsilon)/2\epsilon$ is the normalized pitch angle variable and $\hat{\omega}_b$ is the normalized bounce frequency, such that $\hat{\omega}_b = 1$ at $\xi = 1$. In general, D is a slowly varying function of ξ through $\hat{\omega}_b$. In the small ξ limit, $\hat{\omega}_b = \pi/\ln(16/\xi)$. Plugging Eq. (62) into Eq. (24), we obtain the frequency shift due to the nonadiabatic response of trapped electrons with collision:

$$\frac{\delta\omega}{\omega} = \frac{16\pi^3 \epsilon q_e^2 v_A^2 \sum_l \int (F_e/\omega_b) E dE d\xi (1 - e^{i\sqrt{D}\xi}) (\langle H_e \rangle_l)^2}{m_e^2 c^2 \omega^2 R q T_e \int_{-\infty}^{+\infty} d\theta |\nabla S|^2 \Phi^2}, \quad (64)$$

where the subscript l denotes the l th trapped region in the infinite Fourier θ space. Note that, in the limit of $\bar{\nu}/\omega \ll 1$ considered here, the dominating contribution to the damp-

ing rate (or the imaginary part of $\delta\omega$) comes from a small integration region in $\xi \ll 1$. Thus, in the integration in ξ , we may treat $\hat{\omega}_b$ as a constant and take a characteristic value of $\xi \approx \xi_0$, such that $\text{Re}(\sqrt{D})\xi_0 = 1$, which gives approximately $\xi_0 \approx \sqrt{v/\omega\epsilon}$. The bounce-average term $\langle H_e \rangle_l$ can be likewise calculated asymptotically to give

$$\langle H_e \rangle_l = \frac{2\omega_b(1)}{\ln(16/\xi_0)} \int_0^{\theta_m} \frac{JB d\theta}{v_{\parallel}} [H_{\text{even}}(\theta) - H_{\text{even}}(\pi)] + H_{\text{even}}(\pi) \quad (65)$$

and

$$\sum_l [\langle \bar{H}_l(\theta) \rangle]_{\text{curv}}^2 = \lambda^2 \left(\frac{\pi}{2\Gamma} \frac{1}{[\ln(16/\xi_0)]^2} + c_0 \right), \quad (66)$$

where H_{even} denotes the even part of H_e as a function of $\bar{\theta} = \theta - 2\pi l$, the subscript curv denotes the curvature part of \bar{H}_e , and c_0 is a constant that depends on the value of the magnetic shear s . For typical parameters, the first term in Eq. (66) is greater than the second term, since $\Gamma \sim \epsilon \ll 1$. Thus we may neglect c_0 for simplicity. The corresponding contribution from the parallel electric field term can be similarly calculated. After integrating over ξ and E and taking the imaginary part of $\delta\omega$, we finally obtain an explicit formula for the damping rate γ_e induced by trapped electrons:

$$\frac{\gamma_e}{\omega} = \frac{\sqrt{\pi/8}}{1 + \lambda^2} \left[I_1 \left(\frac{sk_{\theta} \rho_s}{\Gamma} \right)^2 + 8\lambda^2 I_2 q^2 \beta_e \right] \times \sqrt{\frac{v}{\omega}} \left[\ln \left(16 \sqrt{\frac{\omega\epsilon}{v}} \right) \right]^{-3/2}, \quad (67)$$

where I_1 and I_2 are two energy integration factors defined as follows:

$$I_1 = \int_0^{\infty} dz \frac{e^{-z}}{z^{1/4}} \sqrt{Z_{\text{eff}} + \Pi(z)}, \quad (68)$$

$$I_2 = \int_0^{\infty} dz \frac{e^{-z}}{z^{1/4}} (z-2)^2 \sqrt{Z_{\text{eff}} + \Pi(z)}. \quad (69)$$

It is instructive to note that the first term in Eq. (65) comes from the parallel electrical field, and is proportional to $(k_{\theta} \rho_s)^2$, whereas the second term comes from the curvature drift of trapped electrons, and is independent of the mode number. This damping rate given by Eq. (65) is similar to that of Rosenbluth,³² and also Gorelenkov and Sharapov.³¹ However, the logarithm scaling is different from that of Ref. 31. The difference comes from how the bounce-average term $\langle H_e(\theta) \rangle$ is calculated. Gorelenkov and Sharapov³¹ obtained a $\frac{1}{2}$ logarithm scaling by dropping the first term in Eq. (66), and keeping only the second term. Our $-\frac{3}{2}$ scaling is obtained by keeping the first term in Eq. (66), which is larger than the second term for typical parameters.

D. Application to the TFTR NBI experiment

Here we apply our formulation to the TFTR experiment by Wong *et al.*¹¹ Parameters for this experiment are

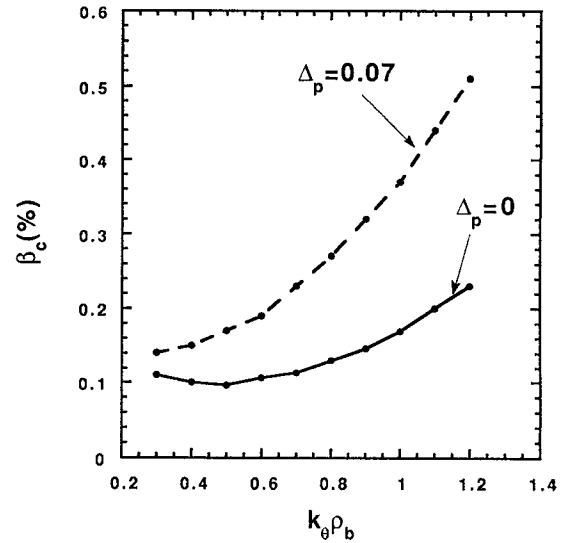


FIG. 12. The critical beam beta value versus $k_{\theta} \rho_b$ for two values of Δ_p at $r=30$ cm for the TFTR TAE experiment.

$R=240$ cm, $a=75$ cm, $B=1.0$ T and injected beam particle energy $E_b=110$ keV. We consider the stability of the TAE modes at $r=30$ cm, where $q=1.32$, $s=0.48$, $n_e=2.7 \times 10^{13}$ cm⁻³, $T_e=1.1$ keV, $\beta_e=\beta_i=1.2\%$, $Z_{\text{eff}}=2.5$, beam density scale length $L_b=18$ cm, and $v_b/v_A=1.1$. For the beam particle distribution, we take a slowing-down energy distribution with zero pitch angle. Thus, only circulating energetic particles are considered.

Figure 12 shows the critical beam beta values versus $k_{\theta} \rho_b$ for two values of Δ_p . The results are obtained by balancing the growth rate induced by beam particles with the sum of ion Landau damping and collisional trapped electron damping. The continuum damping is assumed to be negligible. We find that the collisional trapped electron damping dominates over the ion Landau damping due to relatively small ion beta and large electron collisional frequency. The ion damping rate is calculated to be $\gamma_i/\omega=0.1\%$, while the electron damping rate is $\gamma_e/\omega=[3.9(k_{\theta} \rho_b)^2 + 1.45]\%$, where we have converted $k_{\theta} \rho_s$ into $k_{\theta} \rho_b$ for $\Delta_p=0$. This collisional electron damping is much larger than the usual collisionless electron damping of $\gamma_e/\omega=q^2 \beta_e v_A/v_e=0.27\%$. We note that the electron damping increases quadratically as a function of the mode number. On the other hand, the beam-induced growth rate increases initially for small $k_{\theta} \rho_b$, but saturates at finite value of $k_{\theta} \rho_b=1.0$. Thus, the critical beam beta increases as a function of mode number for a finite value of $k_{\theta} \rho_b$. In particular, for a toroidal mode number $n=2$ that corresponds to $k_{\theta} \rho_b=0.6$, the critical beta is 0.11%. The effect of the finite pressure gradient ($\Delta_p=0.07$) increases the critical beta to 0.2%. This range of the critical beta value is consistent with the experimental estimate of $\beta_c \approx 0.5\%$.

IV. NONLOCAL THEORY

Here, we consider the energetic particle effects in the nonlocal limit and take into account the slow variation of

the envelope function $A(r)$. We start from a quadratic form expressed in the real space. Equation (11) becomes, in the real θ space,

$$\frac{\delta\omega}{\omega} = \frac{2\pi \int J d\theta d\phi dt \int d^3v q_j (\hat{H}^\sigma)^* \hat{h}_j^\sigma}{\omega c^2 \int J d\theta d\phi dt |\nabla_\perp \hat{\Phi}|^2 / v_A^2}, \quad (70)$$

where $\hat{}$ denotes functions in the real space and $t=nq$ is the radial variable. Note that in the real space the integration domain in θ is 2π . Following Zonca and Chen,¹⁶ we write $\hat{\Phi} = \sum_j \delta\hat{\Phi}_j(t) \exp(in\phi - ij\theta)$ and assume the poloidal harmonics $\delta\hat{\Phi}_j(t)$ to have the form $\delta\hat{\Phi}_j(t) = A(t) \delta\hat{\Phi}(t, t-j)$, where $\hat{\Phi}(t, t-j)$ is a function of a fast variable $t-j$ and a slow variable t , while $A(t)$ is an envelope function of the slow variable only. In the spirit of ballooning representation, the fast varying function $\delta\hat{\Phi}(t, t-j)$ is written in terms of its Fourier transform,

$$\delta\hat{\Phi}(t, t-j) = \int_{-\infty}^{+\infty} d\theta' e^{-i(t-j)\theta'} \Phi(t, \theta'). \quad (71)$$

After summing over j , we obtain an alternative expression for $\hat{\Phi}$, given by

$$\hat{\Phi} = \sum_p 2\pi e^{in\phi - i(\theta + 2\pi p)} A(t) \Phi(t, \theta + 2\pi p), \quad (72)$$

where p is an integer to be summed from $-\infty$ to $+\infty$. After plugging Eq. (70) into Eq. (68) and summing over p , we obtain a formula for the nonlocal growth rate $\hat{\gamma}_\alpha$ induced by energetic particles:

$$\frac{\hat{\gamma}_\alpha}{\omega_0} = \frac{\int_{t_1}^{t_2} |A(t)|^2 dt N_\alpha(t, \theta_k)}{\int_{t_1}^{t_2} |A(t)|^2 dt W(t, \theta_k)}, \quad (73)$$

where N_α and W are given in Eqs. (25) and (26). Note that in Eq. (71) the integration domain in θ is infinite due to the summation of p , and θ_k is a function of t to be determined. To solve $A(t)$, we express $A(t)$ in the eikonal form $A(t) = \exp(is'\theta_k dt)$. Zonca and Chen¹⁶ found that the zeroth order θ_k satisfies the local dispersion relation as follows:

$$F(\bar{\omega}, \theta_k, s, \Delta_p) = 0, \quad (74)$$

whereas the next order of θ_k determines $A(t)$ to be

$$A(t) = \frac{1}{\sqrt{\partial F / \partial \theta_k}} \sin\left(\int_{t_1}^t \theta_k(\bar{\omega}, t') dt' + \frac{\pi}{4}\right), \quad (75)$$

where t_1 is one of the two turning points of the local dispersion. It is instructive to make Eq. (59) more transparent by exploiting the relation $W(t, \theta_k) \propto \partial F / \partial \bar{\omega}^2$, Eq. (59) then becomes

$$\hat{\gamma}_\alpha \approx \frac{1}{\pi} \int_0^\pi d\theta_k \gamma_\alpha(t, \theta_k), \quad (76)$$

where $\gamma_\alpha(t, \theta_k)$ is the local growth rate given by Eq. (24). Note that we have considered the \sin^2 term in Eq. (71) has fast variation in θ_k as compared with that of $\gamma_\alpha(t, \theta_k)$ in the limit of $n\bar{\epsilon} \gg 1$, so that the \sin^2 can be effectively replaced by $1/2$. From Eq. (74), we see that the nonlocal growth rate equals the local growth rate averaged over θ_k . Numeri-

cally, we find that the nonlocal growth rate induced by fusion alpha particles is smaller than the local growth rate evaluated at $\theta_k=0$.

V. DISCUSSIONS AND CONCLUSIONS

We have developed a perturbative formulation for the stability of a high- n TAE mode in the presence of Alfvénic energetic particles and fusion alpha particles in tokamak plasmas. Our formulation includes the destabilizing effects of energetic particles and stabilizing effects of thermal electron collisional damping and thermal ion Landau damping. The continuum damping can also be self-consistently included by taking into account the two-dimensional wave structure of the TAE mode. For energetic particles, full finite Larmor radius effects and the main drift orbit width effects are retained by employing a gyrokinetic equation, whereas for thermal ions, the lowest-order FLR terms are kept in the calculation of the parallel electrical field which is important for the collisional electron damping. The continuum damping can also be self-consistently included, by taking into account the two-dimensional wave structure of the TAE mode.

We have studied extensively the parameter dependence of the growth rate of the TAE mode induced by fusion alpha particles in the local limit (i.e., in the limit of translational invariance in the ballooning representation). In this local limit, the growth rate induced by circulating alpha particles is found to increase linearly with the toroidal mode number n for small $k_\theta \rho_\alpha \ll 1$, and decrease as $1/n$ for large $k_\theta \rho_\alpha \gg 1$. The maximum growth rate occurs at $k_\theta \rho_\alpha$ on an order of unity, and is nearly constant for the range of $0.7 < v_\alpha / v_A < 2.5$. The value of the maximum growth rate due to the circulating alpha particles is approximately given by $(\gamma_\alpha / \omega)_{max} \approx -3q^2 r \beta'_\alpha$, where the prime denotes the derivative with respect to the plasma radius r . On the other hand, the trapped alpha particle contribution to the growth rate is dominated by the precessional drift resonance. The bounce resonance contribution is negligible. The growth rate induced by the trapped alpha particles peaks sharply at $k_\theta \rho_\alpha \approx v_A / qv_\alpha$, where the precessional drift resonance occurs for the most energetic particles. The maximum growth rate due to the trapped particles is given by $(\gamma_\alpha / \omega)_{max} \approx \sqrt{2\epsilon} \pi^2 q^2 r \beta'_\alpha J_0^2(v_A / qv_\alpha)$.

The effects of the finite plasma beta are considered. We find that the alpha particle destabilizing contribution is reduced by the effects of finite pressure gradient. In particular, the growth rate induced by alpha particles vanishes as the pressure gradient parameter Δ_p approaches the critical value $(\Delta_p)_{crit}$, where the TAE mode begins to merge into the Alfvén continuum.

The global wave structure is taken into account. In the global theory, the growth rate induced by alpha particles equals the θ_k -averaged local growth rate, and is usually smaller than the local growth rate evaluated at $\theta_k=0$. Furthermore, the continuum damping can be included in the global theory. In order to drive the TAE modes unstable, the destabilizing contribution of energetic particles must overcome the thermal ion Landau damping, the electron

collisional damping, and the continuum damping. As an example, we consider the critical alpha beta for the International Thermonuclear Experimental Reactor³³ (ITER) parameters, taking all the damping mechanisms into account. We take the parameters of $B=4.85$ T, $R=600$ cm, and $a=215$ cm, and consider the following local values: $r=60$ cm, $q=1.0$, $s=0.6$, $n_e=10^{14}$ cm⁻³, $T_e=10$ keV, $T_i=10$ keV, $Z_{\text{eff}}=1.0$, and the alpha particle density profile is $n_\alpha(r)=n_\alpha(0)\exp[-(r/L_\alpha)^2]$ with the scale length $L_\alpha=90$ cm. Using Eq. (56), we find the ion Landau damping due to deuterons and tritons is $\gamma_i/\omega=0.71\%$. The electron collisional damping is evaluated using Eq. (65) and is $\gamma_e/\omega(\%)=0.33(k\varphi_\alpha)^2+0.23$, where we have assumed zero pressure gradient. In the local limit, we find the critical alpha beta for excitation of the high- n TAE mode is $\beta_{ac}(0)=0.5\%$, and the most probable mode number to be excited is $n\approx 6$. In the nonlocal theory, the critical beta value is increased to $\beta_{ac}(0)=1.0\%$ for the local parameters used here. The critical beta value will be further increased due to the finite pressure gradient effect and the continuum damping.

In conclusion, we have presented a comprehensive formulation for the stability of high- n TAE modes by taking into account the destabilizing effects of energetic particles or fusion alpha particles and the stabilizing effects of thermal ion Landau damping, electron collisional damping, and the continuum damping. The alpha particle contribution to the growth rate as a function of $k\varphi_\alpha$ has a maximum at $k\varphi_\alpha$ on an order of unity. For ITER-like parameters, the critical alpha beta $\beta_{ac}(0)$ is on an order of 1%. The detailed parameter studies of the TAE stability for the planned TFTR deuteron-triton (DT) experiment³⁴ and for the ITER will be the subject of a future paper.

ACKNOWLEDGMENTS

We acknowledge useful discussions with L. Chen, H. L. Berk, H. Biglari, J. W. Van Dam, K. L. Wong, and F. Zonca. This work was started at the Centre de Recherches en Physique des Plasmas in Lausanne, Switzerland when one of the authors (G. Y. Fu) was working there.

This work was supported by the Fonds National Suisse pour la Recherche Scientifique and by the U. S. Department of Energy, Contract No. DE-AC02-76-CHO-3073.

¹M. N. Rosenbluth and P. H. Rutherford, Phys. Rev. Lett. **34**, 1428 (1975).

²A. B. Mikhailovskii, Sov. Phys. JETP **41**, 980 (1975).

³C. Z. Cheng, L. Chen, and M. S. Chance, Ann. Phys. NY **161**, 21 (1984).

⁴C. Z. Cheng and M. S. Chance, Phys. Fluids **29**, 3695 (1986).

⁵G. Y. Fu, Ph.D. thesis, The University of Texas at Austin, 1988.

⁶G. Y. Fu and J. W. Van Dam, Phys. Fluids B **1**, 1949 (1989).

⁷C. Z. Cheng, G. Y. Fu, and J. W. Van Dam, in *Theory of Fusion Plasmas 1988*, edited by J. Vaclavik, F. Troyon, and E. Sindoni (Societa Italiana di Fisica/Editrice Compositori, Bologna, Italy, 1989), p. 259.

⁸L. Chen, in Ref. 7, p. 327.

⁹J. W. Van Dam, G. Y. Fu, and C. Z. Cheng, Fusion Technol. **18**, 461 (1990).

¹⁰C. Z. Cheng, Phys. Fluids B **3**, 2463 (1991).

¹¹K. L. Wong, R. J. Fonck, S. F. Paul, D. R. Roberts, E. D. Fredrickson, R. Nazikian, H. K. Park, M. Bell, N. L. Bretz, R. Budny, S. Cohen, G. W. Hammett, F. C. Jobs, D. M. Meade, S. S. Medley, D. Mueller, Y. Nagayama, D. K. Owens, and E. J. Synakowski, Phys. Rev. Lett. **66**, 1874 (1991).

¹²W. W. Heidbrink, E. J. Strait, E. Doyle, G. Sager, and R. Snider, Nucl. Fusion **31**, 1635 (1991).

¹³H. L. Berk, J. W. Van Dam, Z. Guo, and D. M. Lindberg, Phys. Fluids B **4**, 1806 (1992).

¹⁴F. Zonca and L. Chen, Phys. Rev. Lett. **68**, 592 (1992).

¹⁵M. N. Rosenbluth, H. L. Berk, D. M. Lindberg, and J. W. Van Dam, Phys. Rev. Lett. **68**, 596 (1992).

¹⁶F. Zonca and L. Chen (private communication, 1992).

¹⁷L. Villard and G. Y. Fu, "Geometrical and profile effects on toroidicity and ellipticity induced Alfvén eigenmodes," to appear in Nucl. Fusion (1992).

¹⁸D. A. Spong, J. A. Holmes, J.-N. Leboeuf, and P. J. Christenson, Fusion Technol. **18**, 496 (1990).

¹⁹S. C. Guo, J. W. Van Dam, and M. Wakatani, Bull. Am. Phys. Soc. **35**, 2117 (1990).

²⁰G. Rewoldt, Nucl. Fusion **31**, 2333 (1991).

²¹H. L. Berk, B. N. Breizman, and H. Ye, Phys. Lett. A **162**, 475 (1992).

²²R. Betti and J. P. Freidberg, Phys. Fluids B **3**, 1865 (1991).

²³T. M. Antonsen and B. Lane, Phys. Fluids **23**, 1205 (1980).

²⁴P. J. Catto, W. M. Tang, and D. E. Baldwin, Plasma Phys. **23**, 639 (1981).

²⁵M. N. Rosenbluth, D. W. Ross, and D. P. Kostomarov, Nucl. Fusion **12**, 3 (1972).

²⁶X. Q. Xu and M. N. Rosenbluth, Phys. Fluids B **3**, 363 (1991).

²⁷J. W. Connor, R. J. Hastie, and J. W. Taylor, Phys. Rev. Lett. **40**, 396 (1978).

²⁸G. Y. Fu and C. Z. Cheng, Phys. Fluids B **2**, 985 (1990).

²⁹H. Biglari, F. Zonca, and L. Chen, Phys. Fluids B **4**, 2385 (1992).

³⁰A. B. Mikhailovskii and I. G. Shuchman, Zh. Eksp. Teor. Fiz. **71**, 1813 (1976).

³¹N. N. Gorelenkov and S. E. Sharapov, Phys. Scr. **45**, 163 (1992).

³²M. N. Rosenbluth (private communication, 1992).

³³D. E. Post, K. Borrass, J. D. Callen, S. A. Cohen, J. G. Gordey, F. Engelmann, N. Fujisawa, M. F. A. Harrison, J. T. Hogan, H. J. Hopman, Y. Igitkhanov, O. Kardaun, S. M. Kaye, S. Krasheninnikov, A. Kukushkin, V. Mukhovatov, W. M. Nevins, A. Nocentini, G. W. Pacher, H. D. Pacher, V. V. Parail, L. D. Pearlstein, L. J. Perkins, S. Putvinskij, K. Riedel, D. J. Sigmar, M. Sugihara, D. W. Swain, T. Takizuka, K. Tani, T. Tsunematsu, N. A. Uckan, J. G. Wegrowe, J. Wesley, S. Yamamoto, R. Yoshino, K. Young, P. N. Yushmanov, and international contributors, *ITER Documentation Series* (International Atomic Energy Agency, Vienna, 1991), No. 21.

³⁴R. V. Budny, M. G. Bell, H. Biglari, M. Bitter, C. E. Bush, C. Z. Cheng, E. D. Fredrickson, B. Grek, K. W. Hill, H. Hsuan, A. C. Janos, D. L. Jassby, D. W. Johnson, L. C. Johnson, B. LeBlank, D. C. McCune, D. R. Mikkelsen, H. K. Park, A. T. Ramsey, S. A. Sabbagh, S. D. Scott, J. F. Schivell, J. D. Strachan, B. C. Stratton, E. J. Synakowski, G. Taylor, M. C. Zarnstorff, and S. J. Zweben, Nucl. Fusion **32**, 429 (1992).